D16

DROP DYNAMICS IN SPACE

T. G. Wang, M. M. Saffren, D. D. Elleman

Jet Propulsion Laboratory
California Institute of Technology
Pasadena, California

The Jet Propulsion Laboratory (JPL) is planning experiments to be performed in weightlessness to study the dynamics of liquid drops. The liquids will range from superfluid helium through ordinary liquids to molten metals and glasses. These experiments will be carried out in a chamber now being developed at JPL that utilizes the forces and torques produced by acoustic waves excited within the chamber.

Preliminary experiments of short duration (5-20 seconds) are being carried out in the weightless environments provided by NASA drop towers and NASA KC-135 aircraft flown along ballistic trajectories. Experiments are planned which will utilize sounding rockets to provide up to 5 minutes of weightless environment; however, these experiments will eventually require weightlessness of more than 5 minutes duration. None of the current facilities — sounding rockets, drop towers, or KC-135 aircraft — can provide a sustained weightless environment. Ultimately the experiments will be conducted in Spacelab — a manned orbiting laboratory to be flown on the Space Shuttle commencing in 1980. Spaceflight will provide weightlessness over a period of a week or more, allowing truly laboratory-like experiments to be conducted on free liquid drops (and bubbles).

In this paper we first discuss the drop dynamics experiments proposed for Spacelab, and then discuss the acoustic chamber — its operation, and how it is being tested for these and other experiments.

SECTION I

THE DROP ROTATION AND OSCILLATION PHENOMENA (DROP) EXPERIMENT

A. INTRODUCTION

The theory of the dynamics of a free drop has been well studied in the approximation that dynamic quantities deviate linearly from a resting drop. With special exceptions to be discussed below, there is no non-linear theory of the dynamics of a fluid drop. Not only are definitive experiments for the large amplitude behavior of fluid drops lacking but there are few definitive experiments even for linear behavior. This is a consequence of the limitations involved in conducting experiments in an earth laboratory. Among these limitations are insufficient droplet sizes for accurate observation, limited available time for experiments, and perturbing effects due to the method of suspending the droplets.

The proposed drop dynamics experiment will utilize the unique zero-g environment provided by the orbiting space shuttle to investigate the dynamics of a free drop. The results of the proposed experiment will be used to verify existing theory, and to provide the necessary insight for further theoretical development of this subject. The deficiencies of the existing theory, which disregards viscosity, internal flows, virtual mass, and other parameters, are exemplified by the different results of Plateau's system of two immiscible fluids[1] and the Skylab science demonstrations[2]. A more detailed description of these two experiments is given is Section II.

Aside from fundamental interest, a better physical understanding of the behavior of the dynamics of free liquid spheroids is required in many areas of science and technology, as demonstrated by the scope of the program presented at this Colloquium.

B. SCIENTIFIC OBJECTIVES

1. Equilibrium Figures of a Rotating Drop

A rotating fluid in its equilibrium state can sustain no internal flow and so rotates as a rigid body. When subject to gravity and contained in a vessel,

at any angular velocity, the free liquid interface (meniscus) assumes a parabolic shape. When the fluid mass is free, however, the dependence of its shape on angular velocity is far less trivial.

In the proposed Drop Dynamics Module experiments to be performed on the Spacelab mission, the stable equilibrium shape of a rotating drop of fluid will be determined as a function of its angular velocity. Also, the angular velocities at which there is a qualitative change of drop shape (bifurcation points) and the critical angular velocity at which the rotating drop fissions will be determined. A more detailed listing of experiment objectives is given below.

The theory of the equilibrium shapes of rotating fluids began with investigations by Newton[3] on the shape of the rotating earth, and the extensive theory that ensued was that of a free fluid held together by self-gravitation. In a crude attempt to verify this theory, Plateau carried out experiments in 1843 on ordinary rotating fluid drops in a neutral buoyancy tank, although such drops are held together by their surface tension, not by gravitation. His experiments were in rough qualitative agreement with the theory of that time, except for one remarkable difference: one of the stable configurations for a rotating drop was toroidal, not generally thought to be an equilibrium shape for a self-gravitating drop. That it is in fact an equilibrium figure for rotating liquid drops held together by surface tension was not demonstrated until the theory of ordinary rotating liquid drops evolved more than seventy years later when Rayleigh[4] investigated droplets symmetric about the rotation axis (see also Appell[5]). The stability of the simple axisymmetric shapes awaited study by Chandrasekhar[6] and even today the stability of the toroidal and nonaxisymmetric shapes remains virtually unexplored both theoretically and experimentally.

Experimental observation of the behavior of a rotating drop held together by surface tension goes beyond simply testing the existing theory. This theory has in fact been embedded[7] in a grander theory which at one extreme embraces fluid masses held together by their gravity, modelling the stars, and at the other extreme embraces uniformly electrically-charged fluid masses,

modelling atomic nuclei. Consequently, any deviation in the observed behavior of ordinary liquid drops from their predicted behavior would call into question the more all-embracing theory of equilibrium figures of fluid masses. Conversely, if experiments on the equilibrium figures of ordinary drops are in agreement with predictions of theory, this would strongly suggest a unified theory of the dynamics of fluid masses. The observed behavior of ordinary liquid drops would then help to frame the theory of their dynamics and this theory in turn could be extended into the astronomical and nuclear realms. This is one of the ultimate aims of the two proposed sets of experiments. The experiments on rotation and oscillation are precursors to future experiments in which the oscillation of rotating drops will be studied. [Perhaps it is worth interjecting that the experiments are also precursors to ones in which the drops are electrically charged, electrically conducting, dielectric, non-Newtonian, or superfluid; and where external fields are applied (electric, magnetic, electromagnetic, acoustic, or thermal). In addition it is envisaged that multiple drop experiments will be performed in which the interactions of free drops can be observed and these experiments will be based, of course, on what has been previously learned about single drop behavior in externally controlled fields.]

The following discussion presents the current theory of the equilibrium shapes of a rotating fluid drop held together by its surface tension. Rayleigh[4] was the first to calculate the axially symmetric equilibrium shapes. These calculations were extended by Appell[5] who gave a more detailed and elegant description opening the discussion of the dynamics of the change of shape and the stability of these shapes. Chandrasekhar[6] made a definitive study of the stability of the simply connected axisymmetric shapes, and in addition obtained the frequencies of their small amplitude oscillations. Ross[8, 9] reviewed and extended some of the previous work on drops to "bubbles" — fluid drops less dense than the surrounding medium. Gans[10] has examined the small amplitude oscillations about equilibrium shapes of compressible fluids. The equilibrium shape of a drop containing a bubble was discussed by Bauer and Siekmann[11], while Böhme, Johann, and Siekman studied the shape of a rotating dielectric drop in an electric field[12]. Finally, Swiatecki[7, 13], by inserting the theory of the equilibrium shapes of "surface-tension drops" into the more

general theory, was able to give a fairly complete semiquantitative description of the stability of shapes for such drops as a function of their angular momentum, including a discussion of metastable shapes he calls "saddle-point" shapes.

The axisymmetric equilibrium shapes (see Figs. 1 and 2) are conveniently described as a function of the dimensionless angular velocity, Ω , which is the angular velocity measured in units of the fundamental oscillation frequency of the resting drop. [$\Omega = \omega / (8\sigma/\rho a^3)^{1/2}$ where ω is the rotational angular velocity, σ is the surface tension, a is the equatorial radius, and ρ is the density]. When $\Omega < 0.7071$, there are always two equilibrium shapes; the one of lower energy is simply connected, while the other is torus-like. For $\Omega = 0.7070$ there appears an additional "collapsed" shape in which zero thickness at the center yields a "figure-eight" cross section. For $0.7071 < \Omega < 0.73$ there are two torus-like shapes but still two simply-connected shapes. When $\Omega = 0.73$ there is only one torus-like shape[a] but still two simply-connected shapes. The torus-like shapes are lost once $\Omega > 0.073$ and when $\Omega = 0.7540$ there remains only one simply connected shape; this is the greatest angular velocity that an axisymmetric equilibrium shape can have.

The only detailed study of the stability of the equilibrium figures was made by Chandrasekhar[6] but only for the simply connected shapes. He showed that for $\Omega = 0.584$ the drop can deform, without changing its energy, to another shape not having rigid body rotation; thus the original shape is unstable. He presumes that the stable equilibrium shapes become nonaxisymmetric for $\Omega = 0.584$. This presumption is based on an analogy with what is known to occur for a liquid mass held together by self-gravitation. There the stable equilibrium figures are true ellipsoids below a critical angular velocity and triaxial ellipsoids above.

As shown in Fig. 3, at $\Omega = 0.584$ (the bifurcation point), the secular stability passed from the sequence of axisymmetrical shapes to triaxial shapes. Berringer and Knox[14] have calculated that for the "surface-tension" drops the

---

[a] Appell[5] and Ross[8] disagree on the number of toroidal shapes for $\Omega < 0.7071$.

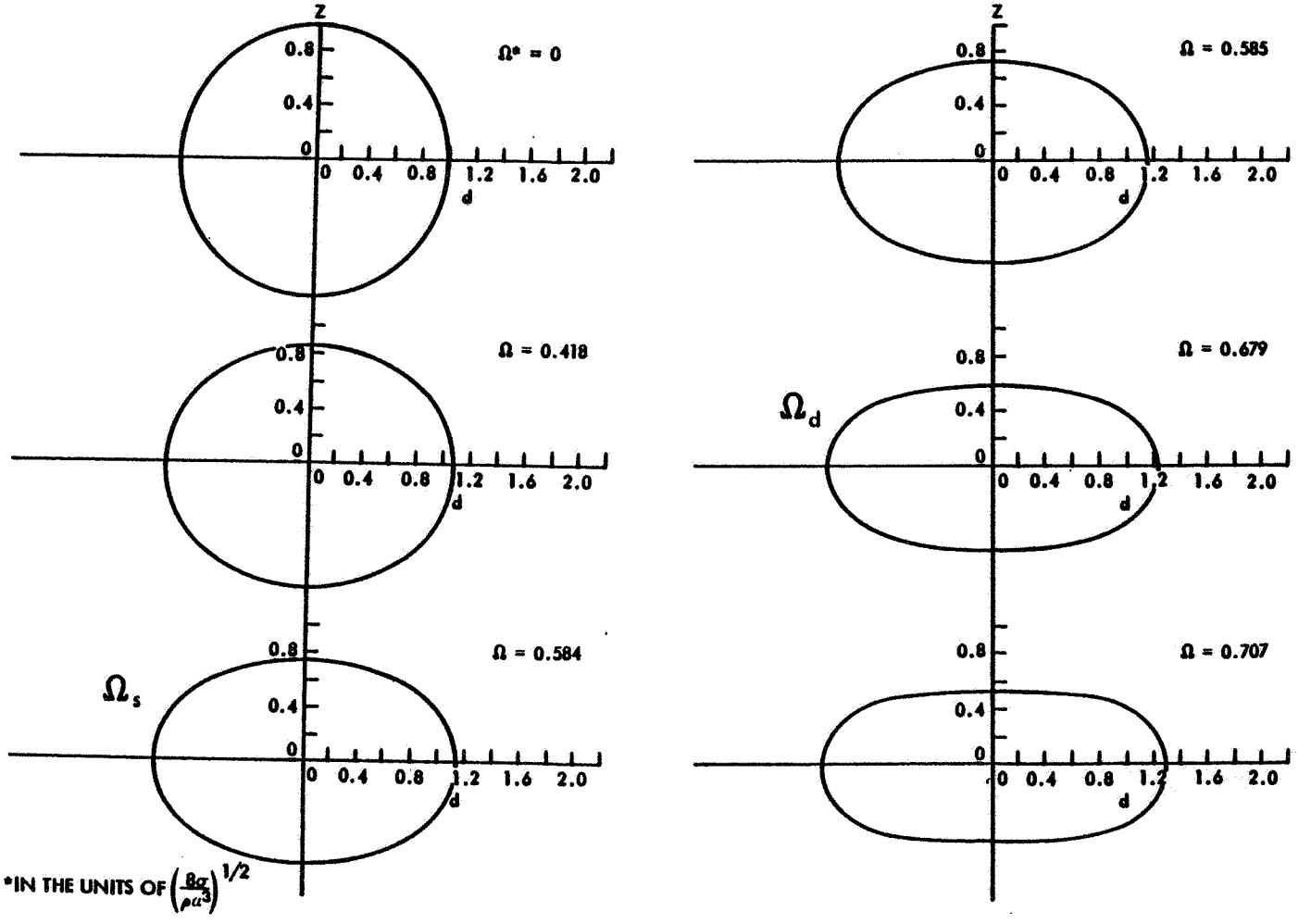

Fig. 1. Axisymmetric Equilibrium Shapes

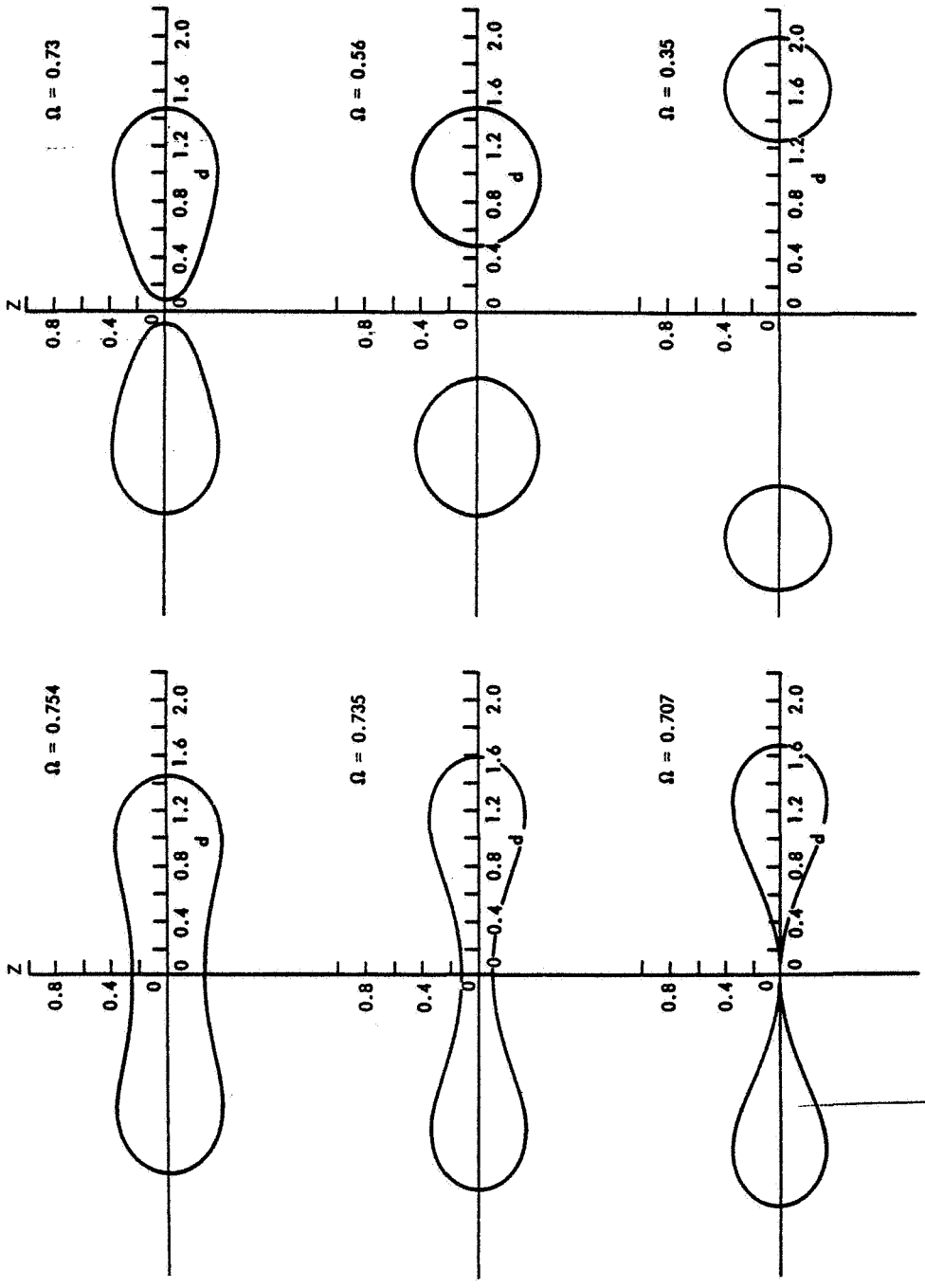

Fig. 2. Axisymmetric Equilibrium Shapes (to Pinch-Off)

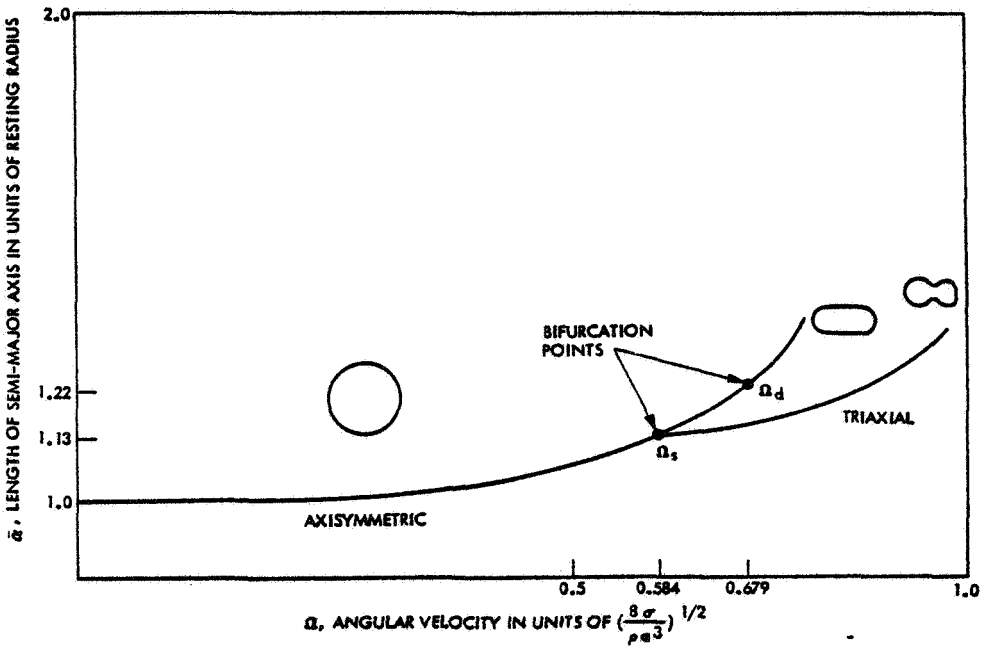

Fig. 3. Illustration of Bifurcation Points

triaxial shapes are not ellipsoids, but the stability of the toroidal shapes has received no definitive treatment. However, the results of Wong[15] on the toroidal shapes of charged liquid drops suggests that these equilibrium shapes may be "saddle-shapes" — shapes stable against deformations that preserve the axial symmetry but unstable against others such as varicose deformation against which fluid jets are unstable (the Rayleigh instability). The triaxial equilibrium saddle-shapes were calculated by Pik-Pichak[16].

The neutral buoyancy experiments of Plateau[1] on the shapes of rotating liquid drops are in qualitative accord with the transition from axisymmetric to triaxial shape as theoretically described by Chandrasekhar[6]. However, Plateau showed that at high angular velocity the drop first rotates nonrigidly and a toroidal shape is then obtained which becomes a rigidly rotating figure, indicating that the toroidal shape is indeed stable. However, this conclusion was called into question by very recent experiments by the authors at JPL which

showed that if the drop is of the less viscous fluid rather than the more viscous as it was in Plateau's original experiment, the toroidal shape is not stable, pinching off as does a liquid jet.

The Skylab experiments on rotating drops[2] yielded the "pinched" triaxial shapes resembling "dog-bones." In one experiment a dog-bone shape fissioned; the reason for this was not clear. The particular dog-bone may actually have been a "saddle-point" shape, or an internal flow or slight oscillation within a stable shape close to the limit of stability may have converted it to a "saddle-shape" when the extra energy was added to the rigid body's fluid motion.

It is very important to note that the Plateau and Skylab experiments yielded different shapes for sufficiently large angular velocity — there was no dog-bone shape demonstrated in the Plateau experiments, nor was there a toroidal shape demonstrated in the Skylab experiments. Similar discrepancies were noted in experiments on cylindrical liquid columns rotating about their axes. Neutral buoyancy experiments carried out by Carruthers[17] showed the instability of such columns always to be axisymmetric, while the Skylab experiment on rotating liquid columns showed the instabilities to be nonaxisymmetric[17]. However, the axisymmetric instabilities were recovered on Skylab once the fluid was made sufficiently viscous.

Plateau's failure to observe the dog-bone may have been due to the effect of "added mass"[b], i.e., in the Plateau experiment a triaxial drop nonaxisymmetric about the rotation axis will entrain adjacent portions of the surrounding liquid (Fig. 4). The consequence of this added mass is to severely modify the pressure drop across the droplet interface. In the limit that the adjacent fluid moves rigidly with the droplet, the pressure drop vanishes. In this extreme, the protions of the droplet that extend into the added fluid will tend to assume a spherical shape to minimize the surface energy. In fact, examination of the shapes obtained by Plateau for rapid rotation do indeed show such "spherical caps" (see Fig. 4).

---

[b] Also know as virtual mass or hydrodynamic mass.

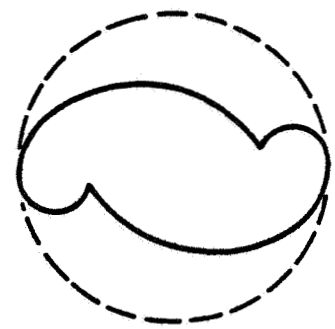

Fig. 4. The solid lines indicate the shape obtained by Plateau. The dotted lines suggest the "boundaries" of the added host liquid

In weightlessness the added mass effect becomes negligible because the ratio of the density of two fluids can be chosen to be three orders of magnitude less than unity.

Thus it appears that viscosity and virtual (added) mass effects strongly limit the validity of neutral buoyancy experiments. In fact, their effects on the flows in rotating fluids may make otherwise stable shapes unstable and vice versa (the "spin-up" effect associated with Ekman boundary layers)[18]. These problems can be studied experimentally only in the true weightlessness afforded by space flight where the viscosity and the density differences of the two liquids can be freely chosen.

2. Large Amplitude Oscillation of a Liquid Drop

In contrast to the problem of a rotating drop, a reasonably complete theoretical formulation of small amplitude dynamics of freely-suspended liquid drops under the influence of surface tension forces has been well developed[19-24]. A rather extensive review of the theoretical work has been given by Chandrasekhar and a large variety of experimental tests have been conducted to verify and support this theoretical work. The experimental procedures fall into three general categories: the liquid drop is suspended in a neutral buoyant media, the drop

is supported by a vertical gas flow, or the drop falls through a gas or vacuum. All of these methods suffer various limitations which have made a detailed quantitative comparison of theory and experiment limited in scope.

At the present time there is no adequate theory for large amplitude oscillations of liquid drops, nor have the criteria for rupture or coalescence of liquid masses and the transition region between the high viscosity and low viscosity regions been developed. However, Foote[25] and Alsonso[26] have simulated with computer calculation the motion of a drop undergoing large amplitude oscillation.

In 1879 Lord Rayleigh conducted one of the first investigations on the behavior of an oscillating liquid drop about its spherical equilibrium shape. He limited his study to the case where the oscillations were axisymmetric and assumed that the internal motions were described by a potential flow field. He did not include viscous effects. The results of Rayleigh's investigations can be expressed by a series of expansion of Legendre polynominals:

$$r = a_0 + \Sigma\ a_n P_n(\cos\theta) \tag{1}$$

where r is the radial coordinate, ρ is the polar angle measured from the pole of the drop and the coefficients a_n are functions of time.

In solving for the a_n's that appear in Equation (1), it is necessary to limit the oscillations to small amplitudes, $a_n << a_0$. It can be shown that if $a_n \cong \cos \omega_n t$ then

$$\omega_n^2 = n(n-1)(n+2)\ \frac{\sigma}{\rho a^3} \tag{2}$$

where σ is the surface tension, ρ is the density of the liquid, and a is the equilibrium spherical radius. It should be noted that n = 0 and n = 1 correspond to rigid body motions. The fundamental mode of oscillation is given by n = 2. The period for the fundamental mode is given by

$$\tau_2 = \pi \sqrt{\frac{\rho a^3}{2\sigma}} \tag{3}$$

For a 2.5-cm diameter water drop where ρ = 1 gm/cm^3 and σ = 75 dyn/cm, the period would be τ_2 = 0.36 sec for the fundamental mode, τ_3 = 0.19 for n = 3 and τ_4 = 0.12 for n = 4.

Foote[25] has carried out rather extensive computer calculations of Rayleigh's equation and has dropped the restriction of the calculations to small amplitudes. The results of Foote's calculations are shown in Fig. 5, for the cases of n = 2, 3 and 4. In all cases the drop is started in motion at time T = 0 in the deformed shape with the internal flows at zero. The time is measured in units of π radians so at T = 1 the drop has gone through one-half of a cycle. Even at large amplitudes the calculated shape of the drop appears to have the approximate shape observed in experiments[25]. A detailed comparison with experimental data[25] is not possible because the quality of the data is limited by the experimental techniques that are now available. It should also be pointed out that the Rayleigh solutions are probably only true for amplitudes corresponding to T from 0.375 to 0.625[25].

In the analysis that has been discussed so far, viscous effects have not been included. Lamb[20] has shown that for small viscosity the only effect on the oscillating spherical drop is the gradual damping of the amplitude of the oscillation. The normal mode frequency is not affected by the viscosity. The decay of the amplitude A can be shown to be given by

$$A = A_0 e^{-\beta_n t} \tag{4}$$

where A_0 is the initial amplitude of the oscillation of the drop and β_n is given by

$$\beta_n = \frac{(n-1)(2n+1)\nu}{a^2} \tag{5}$$

where ν is the kinematic viscosity of the liquid and a is the radius of the drop. For a drop of water 2.5 cm in diameter with ν = 0.014 cm^2/sec oscillating in fundamental mode n = 2 then β = 0.045. Thus a free oscillating drop would decay to 1% of its initial amplitude in 102 sec.

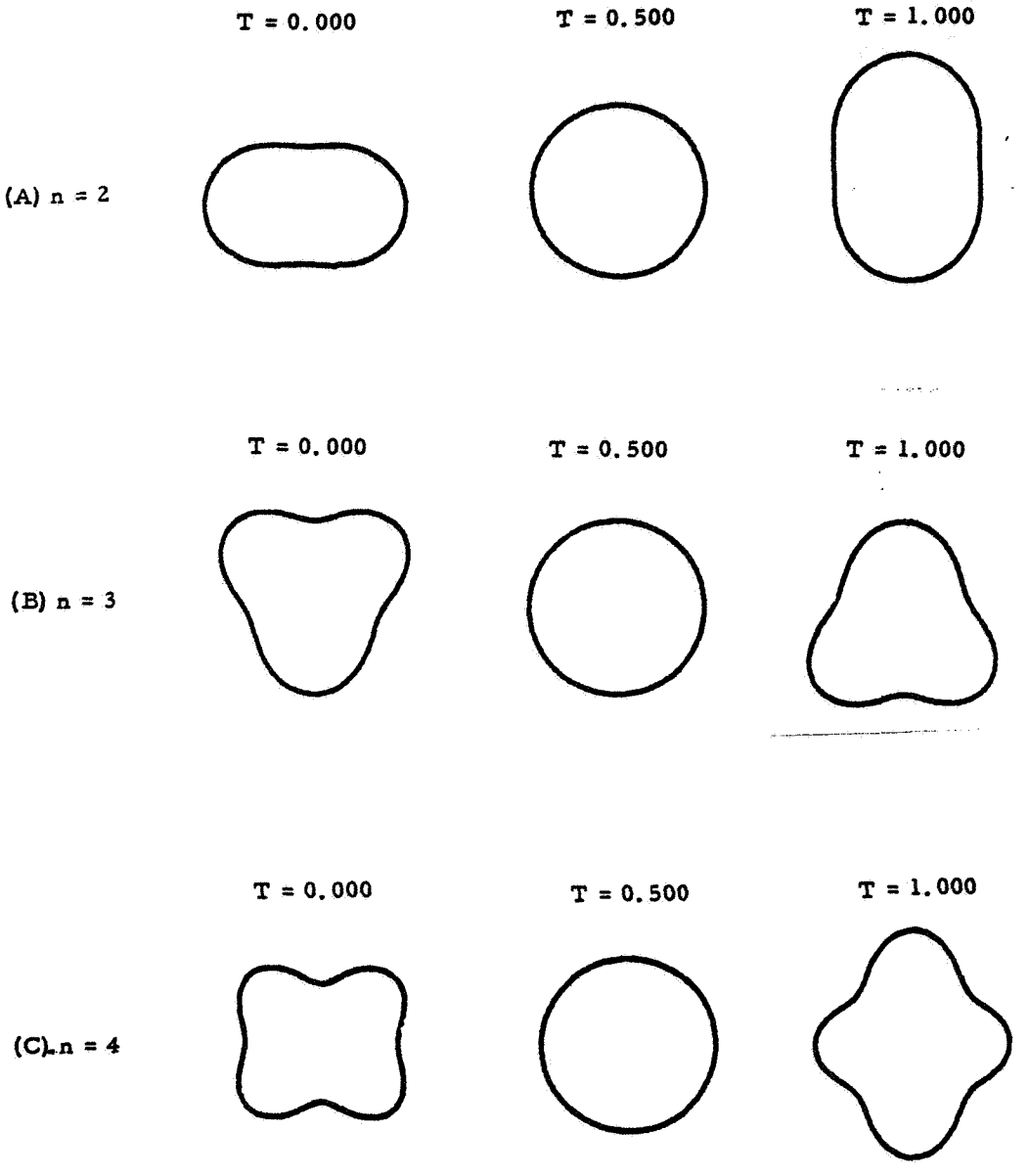

Fig. 5. Fundamental Modes of Oscillation
(The axial ratio is 1.7 at the maximum distortion and the axis of symmetry is vertical)

Chandrasekhar[24] has shown that aperiodically damped motion of the drop is possible for the fundamental mode if $\omega_n a^2/\nu$ is less than 3.69 cm^2/sec. Therefore a drop 0.023 cm in radius or smaller would experience aperiodic motion. Prosperetti[27] has found that a drop that is initially critically damped should have an aperiodic decay for a short time and a damped oscillation motion at a later time. He implies that the effective damping factor first increases and then decreases with time. These predictions have yet to be verified by experiment.

In contrast to the case of small viscosity where ω_n is independent of viscosity, Happel[23] and Chandrasekhar[24] have shown that for a system controlled by gravitational forces as $\nu \to \infty$ the normal mode oscillation can be given by

$$\omega = \omega_n^2 \frac{2n+1}{2(n-1)(2n^2+4n+3)} \frac{a^2}{\nu} \tag{6}$$

where a is the radius of the sphere and ν is the kinematic viscosity.

Foote has noted from his computer calculations that the drop spends more time in the prolate configuration than in the oblate (57% vs 43%). Montgomery[28] has made vertical wind tunnel measurements on drops and has observed a similar behavior. However, it is not clear how much effect the air streaming around the drop has on this unequal distribution of time in the prolate and oblate shapes. At small amplitudes the calculations show that the drop spends an equal amount of time in the two configurations.

Another feature of the computer calculation is that the period of oscillation is not constant with large amplitude oscillations but shows an increase in the period as the amplitude is increased. For a large oscillation in which the axial ratio, γ, and the ratio of major to minor axis is 1.7, the fundamental frequency increases approximately 9% for an ellipsoidal drop. If the calculation is done for a Rayleigh-shaped drop, the predicted increase is about 5%.

Montgomery's[28] experimental work on small drops agrees qualitatively with these computer calculations. The computations show a rather smooth change in the increase of the period with increasing amplitude of the oscillation.

The calculations do not take into account any turbulent flow within the drop which one might expect to find at large amplitude oscillations. This turbulent flow might very well manifest itself as a break in the curve of period vs amplitude as one enters the turbulent flow region.

As the drop oscillations grow to larger amplitudes a point is reached when fission of the drop is possible. A considerable amount of theoretical work on charged drops has been stimulated by nuclear physicists' attempts to model nuclear fission with the behavior of a charged drop. Diehl[29] has calculated the ternary fission for the liquid drop model and has shown that there are two modes of fission, the prolate mode that has axial symmetry and the oblate mode. Alonso[26] has calculated the binary fission case and finds that the neck connecting the two sections becomes very elongated and eventually develops a long thin neck that will not pinch off until it has extended to virtually no width. It has been hypothesized that the pinch-off is actually initiated by a surface fluctuation in the neck. Thompson and Swiatecki conducted a neutral buoyant experiment on polarized drops and observed the thin-necking. In addition, from their data it appeared the drop was attempting fission in the prolate ternary mode.

The liquid drop can undergo another type of oscillation that has received little attention to date. That is the so-called running wave, which for the fundamental frequency is the superposition of fundamental oscillations along the x and y axes $\pi/2$ out of phase with one another. A careful investigation of film taken by the astronauts on Skylab of oscillating drops seems to indicate that this type of oscillation was indeed stimulated. A more detailed investigation of this type of behavior is needed, particularly in the large amplitude regions. One could then determine whether the running wave is still a superimposition of the fundamental modes.

As one can see there has been rather extensive theoretical work carried out on small amplitude oscillation and a considerable number of computer calculations on large amplitude oscillations and fission processes. Unfortunately, the experimental work needed to back up these calculations, even though extensive, has been limited by various experimental constraints.

The experimental techniques used to date fall into four general categories. The first technique is the suspension of a liquid drop in a viscous neutral buoyant medium[30-34]. However, the energy dissipation mechanism for a droplet oscillating within another fluid of appreciable density has been shown by Miller and Scriven[30] to be significantly different from the case in which the second fluid has negligible density. Also, it was pointed out by Park and Crosby[35] that the interfacial tension is modified by the presence of the second medium.

The second technique is the suspension of a liquid droplet in gas currents or electrical fields[28]. Unfortunately, experiments with droplets in air or electrical fields have generally been limited to drop sizes in the millimeter diameter range where it has been difficult to obtain accurate quantitative information for comparison with hydrodynamic theory[35]. In addition, the oscillations in a column of gas supporting the drop may create forced vibrations in the drop[33].

The third technique involves the drops free-falling through a gas or vacuum such as the experiments carried out in the NASA MSFC 400-foot drop tower. These experiments have shown that it is possible to obtain accurate data on shape oscillations of liquid masses deployed in sizes in the centimeter to several centimeter diameter range when the liquids are deployed under carefully controlled conditions with relatively low internal vorticities. Unfortunately, good quantitative resolution in terms of fundamental modes have not been obtained due to the very short (3 second) experiment times available.

Recently, Skylab astronauts have demonstrated the capability of performing drop dynamics experiments in space. Although those experiments were carried out in uncontrolled and unrestrained conditions, the results have already stimulated a great deal of interest both in the scientific community and in the public[2].

This discussion emphasizes the need for a quantitative experiment on oscillation of drops that is free from all the defects mentioned above.

SECTION II

APPARATUS

The photograph in Fig. 6 shows one of the laboratory prototypes of the triaxial acoustical levitation resonance chamber[36] that will be used to position and control large liquid drops in zero-g environments. The chamber itself is nearly cubical with inside dimensions of 11.43 x 11.43 x 12.70 cm, which are the x, y and z faces, respectively. Three acoustic drivers are rigidly fixed to the center of three mutually perpendicular faces of the chamber. During operation of the chamber, each driver excites the lowest-order standing wave along the direction the driver faces.

In a resonant mode, the ambient pressure is maximum at the nodes of the velocity wave and minimum at the antinodes. Consequently there is a tendency for introduced liquids and particles to be driven toward the antinodes where they collect and remain until excitation ceases.

Calculation of the acoustic pressure on the drop is simplified by the fact that the characteristic impedance of the liquid $\rho_\ell c_\ell$ is very much greater than that of the gas, ρc,

$$\frac{\rho_\ell c_\ell \ (\sim 10^5 \text{ cgs})}{\rho c \ (\sim 40 \text{ cgs})} \simeq 10^3, \tag{7}$$

where ρ_ℓ and ρ are the density of liquid and gas, respectively, and c_ℓ and c are the sound velocity of liquid and gas, respectively. Because of this impedence mismatch, the acoustic power in the drop is three orders of magnitude smaller than in the gas and is negligible. This simplifies the expression for the radiation pressure $<\Delta P>$ which is time independent and is given at the boundary by

$$<\Delta P> = \frac{\overline{P^2}}{2\rho c^2} - \frac{1}{2}\rho \ \overline{\bar{U}^2} \tag{8}$$

where P is the excess acoustic pressure, $\bar{U}$ is the gas particle velocity, and the bar over a quantity denotes the time average of the quantity. Equation (8) is the "Bernoulli equation"[36-38] which gives the acoustical perturbation on the ambient pressure from its quiescent value.

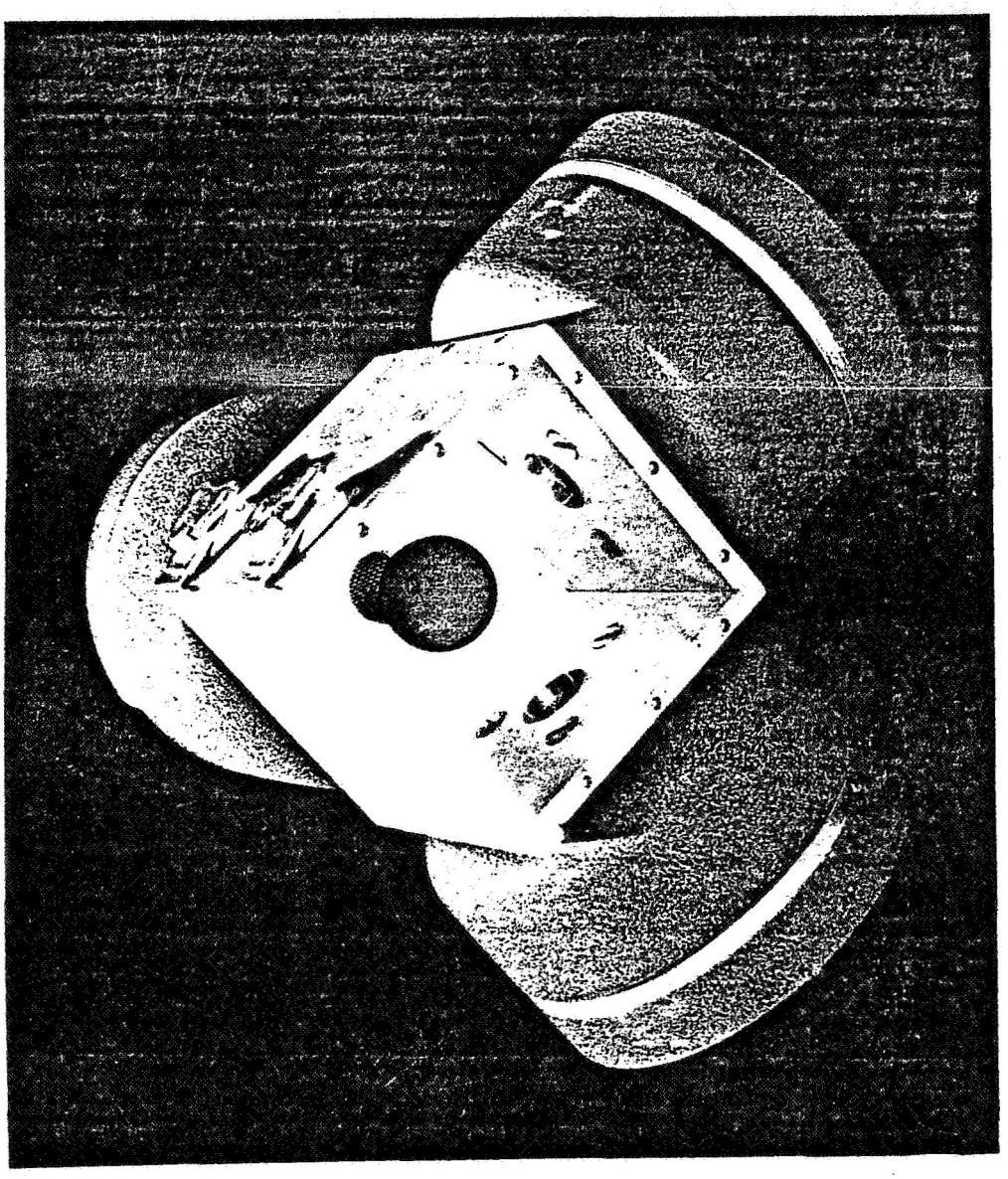

Fig. 6. Acoustic Chamber

The pressure profile in our system can be derived as follows.

The velocity potential ϕ of the wave in the chamber can be expressed as

$$\phi = \phi_x \cos(k_x x) e^{i\omega_x t} + \phi_y \cos(k_y y) e^{i\omega_y t} \tag{9}$$

$$+ \phi_z \cos(k_z z) e^{i\omega_z t}$$

where $\phi_{x,y,z}$ are the complex velocity potential amplitudes of standing waves of frequency $\omega_{x,y,z}$ and wave number $k_{x,y,z}$.

The particle velocity U by definition is

$$\vec{U} = \nabla\phi \tag{10}$$

The pressure is given by

$$P = -\rho\dot{\phi}$$

Fig. 7 shows the resulting expression (Equation 8) for the radiation pressure with only one of the three drivers on ($\phi_x = \phi_y = 0$). The node is a plane ($z = \ell_z/2$), becoming a point when all three are turned on. The profile of Fig. 7 has been verified experimentally.

Because this is a three-dimensional system with independent control on each dimension, it has a great deal of versatility. It can acoustically position a drop, and manipulate a drop once it is positioned; for example, it can induce drop oscillation and/or rotation.

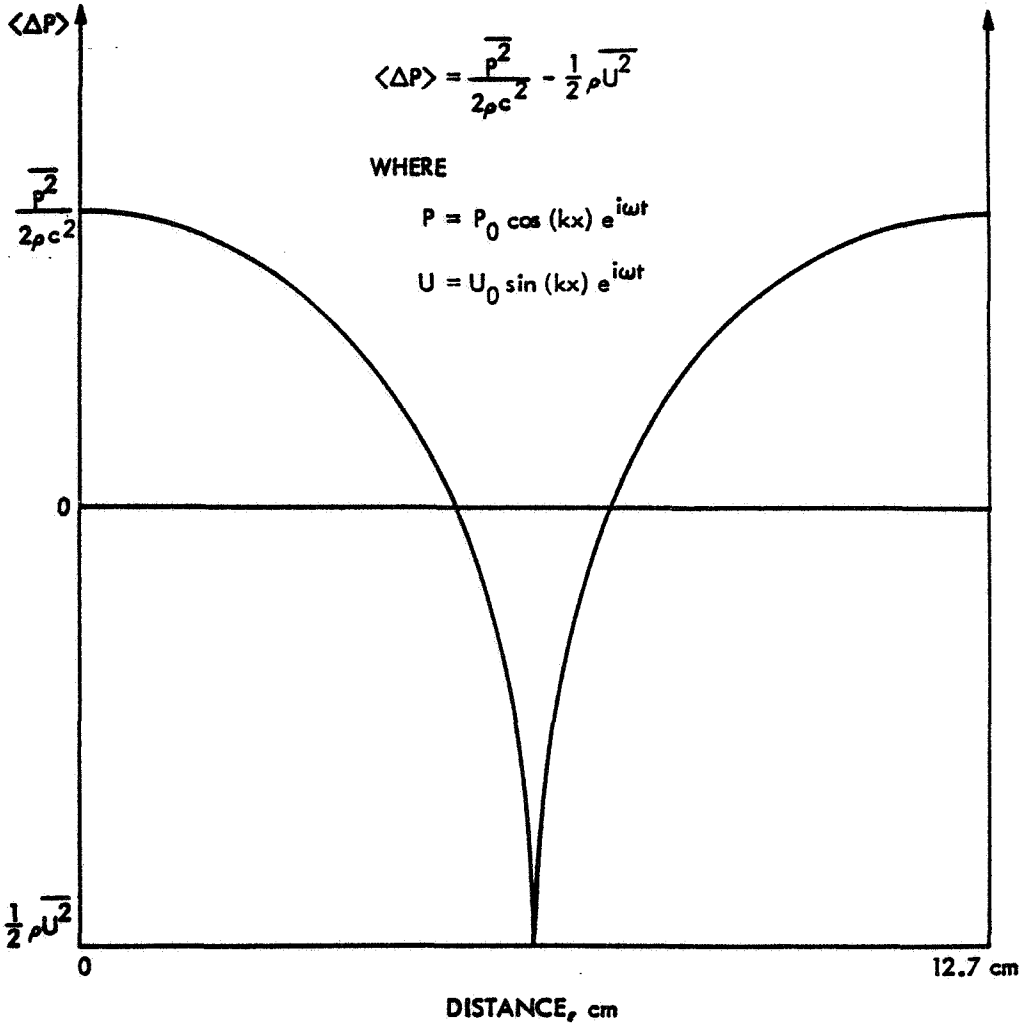

Fig. 7. Theoretical Pressure Profile in the Chamber

SECTION III

OPERATION OF THE CHAMBER

A. ROTATION AND OSCILLATION EXPERIMENTS

In the following discussion, we discuss the operating characteristics of the acoustic chamber necessary to perform rotation and oscillation experiments. Assume that the sample to be studied is a 1.25 cm radius (a) water droplet, the residual acceleration is 10^{-1} cm/sec^2 (10^{-4} g), and the quality factor (Q) (defined as $\omega/2\Delta\omega$) of the acoustic chamber is ~ 25.

a) Newton's equation for the motion of a water drop in an acoustic pressure field is

$$\int \langle \Delta P \rangle \hat{n}_x \, dA = \rho_\ell \cdot 10^{-4} \text{ g} \cdot \frac{4}{3}\pi a^3 \tag{11}$$

In the limit of $ka \ll 1$, this has been calculated by L. V. King[39] to be

$$\frac{P^2}{2\rho c^2} \sin 2kx \cdot 2\pi a^3 \cdot k \cdot \left(\frac{5}{6}\right) = \rho_\ell \cdot \frac{4}{3}\pi a^3 \cdot 10^{-4} \text{g} \tag{12}$$

For a sphere of 2.5-cm diameter, density of 1 gm/cm^3, the corresponding minimum acoustic pressure required to position the drop is

$$P \simeq 10^3 \text{ dyne/cm}^2 \simeq 134 \text{ db} \tag{13}$$

where the decibels (db) are measured against the reference effective pressure (2×10^{-4} dyne/cm^2). For a 50 percent efficient compression driver, less than 0.2 watt of electrical power is needed to provide the required acoustic pressure.

It is worth pointing out that at this acoustic pressure level, the surface tension force (F_s) which acts on the water drop is two orders of magnitude larger than the acoustic force (F_A):

$$\frac{F_s}{F_A} = \frac{\sigma \cdot 2\pi r}{\int \langle \Delta P \rangle \cdot \hat{n}_x \cdot dA} \sim 100 \qquad (14)$$

b) If the amplitude of the above 134 db acoustic wave is modulated at a given frequency ω_o, the drop experiences a modulated force

$$F_o = \int \langle \Delta P \rangle \, n_x \, dA = (\sim 1 \text{ dyne}) \qquad (15)$$

When ω_o matches the normal oscillation modes of the drop given by $\omega_n^2 = n(n-1)(n+2)(\sigma/\rho a^3)$ the amplitude A of the oscillation, assuming potential flow inside the drop, can be as large as

$$|A| = \left| \frac{F_o}{i\omega_o M_\ell \cdot \beta_n} \right| = (\sim 1 \text{ cm}) \qquad (16)$$

where β_n is the damping constant of the nth mode of the drop and M_ℓ is the mass of the drop. Since the drop radius itself is 1.25 cm, this modulation force is sufficient to drive the drop into large amplitude oscillation at least at the fundamental frequency. However, a higher power modulation is required for higher modes due to the increase in damping. That there is in fact sufficient power to do this has been demonstrated in KC-135 flights where the prototype was able to shatter a water drop of 1.25-cm radius in less than one second operating at the fundamental frequency.

c) If the phase between the two orthogonal 134 db waves on the x and y axes is locked with 90° phase shift, this will produce a torque that spins the drop. In the asymptotic limit, the drop will achieve a rotational velocity of 23 rad/sec, exceeding the maximum rotational velocity (10.1 rad/sec) required for this experiment. However, in order to spin up the drop at a constant acceleration, the acoustic power must ramp up as the square root of the rate. The power setting and the rate of increase will have to be determined after the liquid has been selected.

We have demonstrated the rotation capability in our laboratory with a 1.25-cm radius styrofoam ball levitated in a 155 db sound field as presented in Fig. 8. Spinning up of a 1-cm diameter water droplet has also been shown in KC-135 flights.

B. OPERATION OF THE CHAMBER AT EXTREME TEMPERATURES

In future space flights, experiments to be carried out will be extended beyond those on room temperature droplets. These future experiments will require the manipulation and control of liquid helium droplets and of molten metal droplets and glass. In this section we describe laboratory tests of the chamber that demonstrate the feasibility of operation at such temperatures.

a) For the acoustic chamber to operate and function properly between these extreme temperature limits, it must be able to maintain resonance at all times. In fact, the resonant frequencies, f_n, of the chamber are

$$f_n = \frac{nC_o}{2\ell}\sqrt{\frac{T}{273}} \tag{17}$$

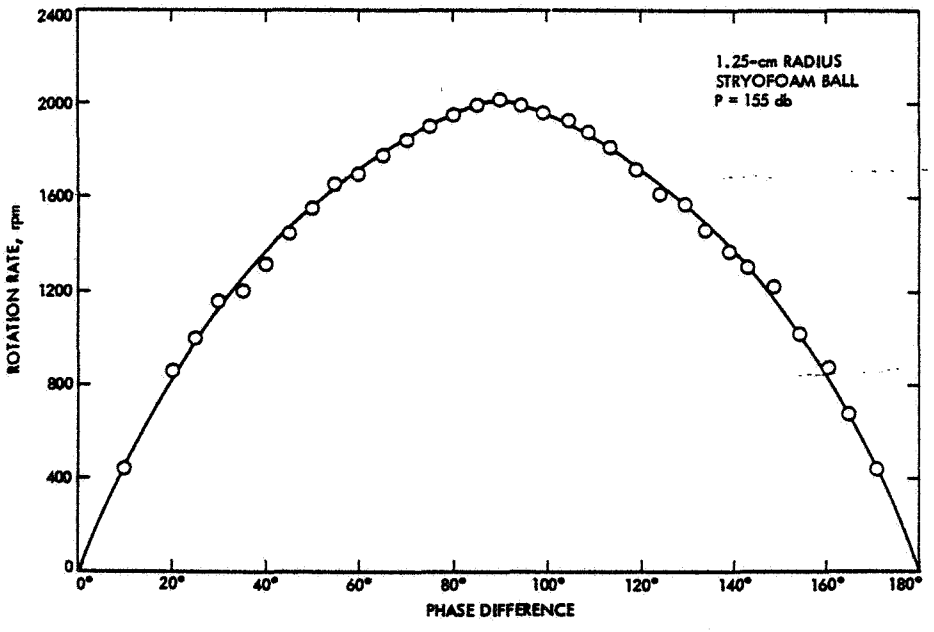

Fig. 8. Rotational Rate as a Function of Phase Difference

where C_o is the velocity of sound at 0°C, ℓ is the physical dimension of the chamber, n is an integer and T is the ambient temperature of the chamber in degrees Kelvin.

An automatic frequency control to maintain resonance despite temperature excursions within the chamber has been developed. The heart of this control is a phase locking loop. The complex displacement X for a system undergoing forced oscillation is

$$X = \frac{-j\, F e^{j\omega t}}{\omega \left[R_m + j\,(\omega m - s/\omega)\right]} \tag{18}$$

where F is the driving force, R is the resistance, m is the mass, and s is the "spring" constant. Without solving the real part of this equation, one can easily see that a resonance occurs where $\omega m = s/\omega$; the complex displacement X lags the driving force by 90°. This is a well known property of acoustical systems. The principle of phase locking is to monitor the driving frequency so that the input signal has 90° phase lead with respect to the acoustical signal inside the chamber at all times.

At the present time we do not have at our disposal acoustical drives that will operate at the high temperatures at which we wish to test the automatic frequency controller. Consequently the variation of high temperatures within the chamber was simulated by mixing helium gas with air to vary in time the resonant frequency in the chamber. The resonant frequencies, f_n, of the chamber are

$$f_n = \frac{nC_o}{2\ell}\sqrt{\rho_o/\rho} \tag{19}$$

where C_o is the velocity of sound in air, ℓ is the physical dimension of the chamber, n is an integer, ρ_o is density of air, and ρ is the density of the air and helium mixture. One can easily see from Equations (17) and (19) that a decrease in the density of the mixture will simulate an increase in the temperature of the chamber. In the test, helium gas was bled into the chamber while a styrofoam ball was being levitated. The purpose of the test is to see how fast the servo loop can track the change in resonant frequency as the "temperature" is varied.

The test was conducted by changing the gas in the chamber from 100% air through intermediate mixtures to a 100% helium composition. This variation in gas density and the resulting change of velocity of sound simulated a change of temperature from 25°C to approximately 2000°C. The fundamental resonance frequency of the chamber thus varied from 1.5 to 4.2 kHz during the simulated temperature rise. The automatic controller was able to vary the driver frequency to match the change in the chamber's resonance frequency, and measurements of the pressure profile in the chamber indicated that the profile maintained its original pattern throughout the test. The most significant portion of the test was the demonstration that the levitated sphere located at the center of the chamber remained at this position throughout the test with no measured motion or oscillation. This indicated that no unwanted oscillation was occurring in the servo system.

b) Another test is the operation of the chamber when the temperature within is highly nonuniform. In a zero-g environment, gravitation-induced convection is absent, leading to inefficient heat transfer from a molten drop positioned in the chamber to the wall. Consequently, the temperature around the droplet can be much higher than at the wall. The questions that we must answer are: (1) Will this extreme temperature gradient affect the sound intensity profile? (2) What will the acoustic wave do to the temperature gradient?

The test apparatus was a glass cylinder 60.76 cm long and 15.78 cm inner diameter. At its upper end a disc heater plate of the same diameter was fitted into the cover. A speaker was mounted in the lower opening. The temperature and sound intensity profile were determined first independently and then simultaneously. The results are shown in Figs. 9 and 10.

Fig. 9, plots the measured acoustic pressure as a function of distance with and without the heater on. It shows that resonance was not perturbed by the temperature gradient. Fig. 10 compares the temperature profiles with and without the speaker on. It shows that the acoustic field slightly improved the heat conductivity of gas without much alteration of the shape of the profile. We conclude from these tests that temperature gradients resulting from molten material being positioned will not affect the positioning capability of the chamber nor will the acoustic field significantly modify temperature gradients which would affect the melting and solidification of the material being positioned.

c) A very convenient method of testing the purity of ultra-pure metals is to measure the resistivity of the metal at low temperatures. The resistivity measurements could be made by using eddy current induction techniques on a levitated sample that would obviate the necessity of placing electrical leads on the sample. Measurements of this type are often conducted at temperatures below 2.0°K.

At the other end of the temperature scale, the determination of the purity of ultra-pure metals requires that the chamber perform at a temperature below 2°K. One of the anticipated uses of the acoustic levitation furnace is the growth of ultra-pure single crystals with a minimum number of crystal defects. It would be convenient to be able to grow the crystal and then make subsequent tests on the crystal in the same chamber. It is felt that this type of handling of the material would greatly reduce inadvertent contamination of the sample and eliminate the possibility of producing defects in the crystal through additional handling when transferring from the furnace to another separate test chamber. The combined

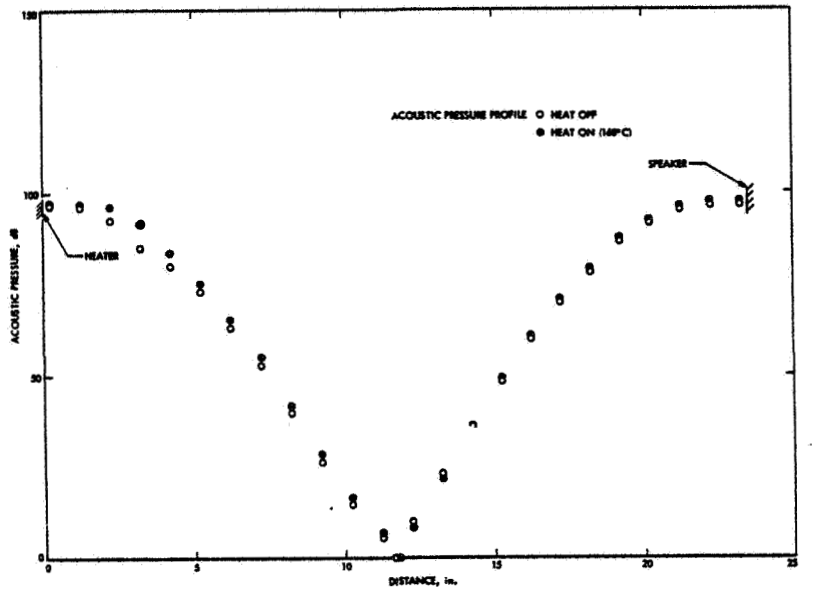

Fig. 9. Acoustic Profile

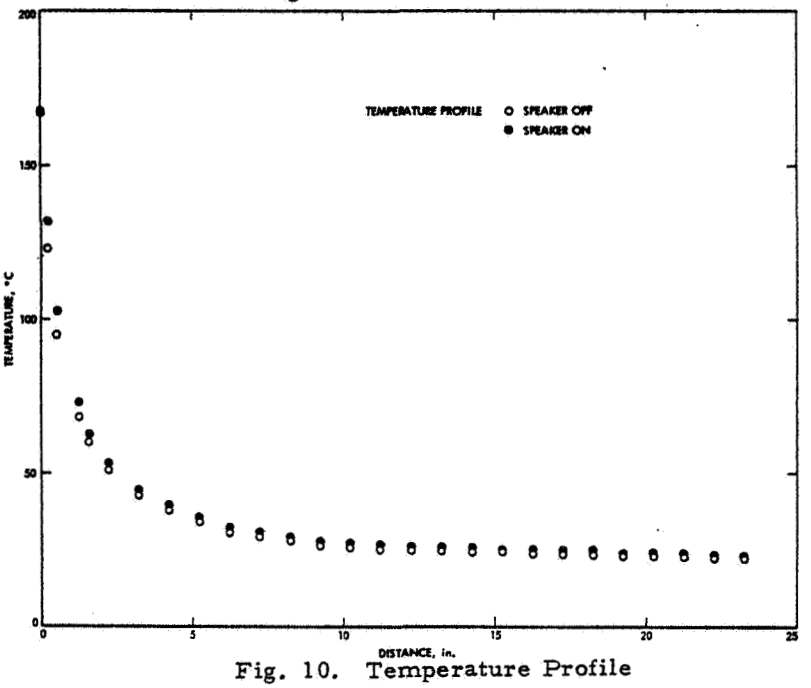

Fig. 10. Temperature Profile

furnace test chamber has the added advantage in that it could reduce the time needed in conducting the purity tests on the samples.

It was therefore decided to conduct exploratory tests on the acoustic levitation chamber at these low temperatures to ascertain any difficulties in operation of the chamber at these reduced temperatures. Preliminary tests were carried out at 1.8°K and the results indicated that the acoustic pattern did not show any significant deviations from room temperature operation.

d) To provide an understanding and engineering design of the flight experiments, it is desirable to study the melting and solidification process under the influence of acoustic fields in an earth laboratory. A high power acoustic chamber that is capable of levitating liquid droplets, glass beads and metal plates in our laboratory has been developed as shown in Figs. 11 and 12.

The capability of the new chamber will be used to make feasibility studies of containerless materials processing in the laboratory, to be carried out with university and industry scientists. Initial tests will be conducted with low-melting organic materials which have the advantages of low density and ease of handling. If these experiments are successful, later tests may be conducted on low-melting metals.

Fig. 11. Acoustically Levitated Water Droplets

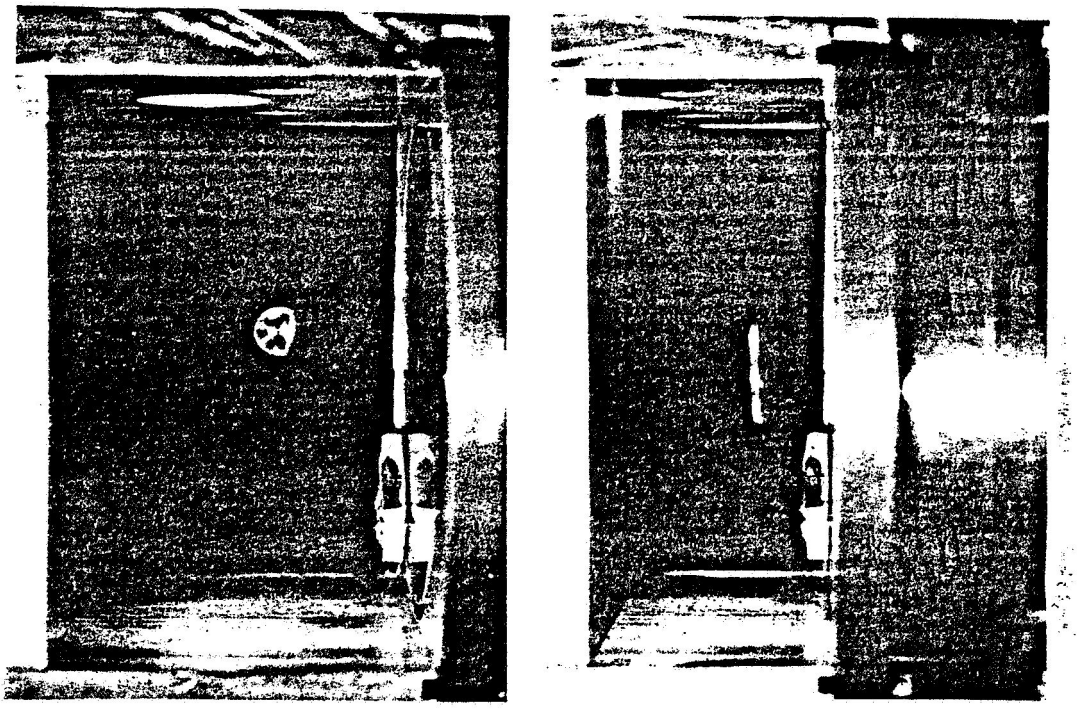

(a) (b)

Fig. 12. Acoustically Levitated Solids: (a) Glass Sphere, (b) Metal Plate